Noncovalent Interactions

Electrostatic Site Attachment of Divalent Counterions to Rodlike Ruthenium(II) Coordination Polymers Characterized by EPR Spectroscopy**

*Dariush Hinderberger, Oliver Schmelz, Matthias Rehahn, and Gunnar Jeschke**

Coordination polymers which are formed from connecting organic bischelating ligand molecules ("ligand monomers") through transition metals have received much attention in the past decade.[1] The use of transition-metal ions such as ruthenium(II) or osmium(II) provides materials with kinetically inert coordinative bonds that are of interest as potential (electro-)optical or magnetic nanomaterials.[1e–h] Such systems are also very well suited as model systems for the study of polyelectrolyte behavior, since they have a well-defined rigid conformation in solution which reduces the complexity of the polyelectrolyte behavior by limiting the conformational degrees of freedom.[2a,b]

Polyelectrolytes are macromolecular substances that are soluble in water or other ionizing solvents.[2] They dissociate into macromolecular ions that carry multiple charges (polyions) together with an equivalent number of ions of small charge and opposite sign. Despite their important role in many fields of scientific research, such as molecular biology (DNA, RNA) and nanotechnology,[3–5] the interplay of electrostatic interactions between macro-ions and counterions is not yet fully understood.[2a,b,6a–6c] Comparison between theoretical and experimental results has proved difficult in the past, as additional complexity is introduced in experiments by solvation effects, specific interaction between counterions and charged groups of the polyelectrolyte, and conformational changes of flexible polymer chains which cannot be separated properly from electrostatic effects.

Herein we consider coordination polymers formed by divalent Ru^{II} ions that are connected by bis(2,2′:6′,2″-terpyridine)-based rigid spacer molecules of variable lengths (Scheme 1) to study the condensation of counterions[6d–g] to a stiff, relatively weakly charged polyion.[6] In the study we use a combination of continuous wave (CW)[7] and pulse[8] EPR spectroscopy on paramagnetic counterions that we have recently used to obtain a local, dynamic picture of counterion condensation to the flexible polyelectrolyte poly(diallyldimethylammonium chloride).[9] For this strongly charged polyelectrolyte we were able to demonstrate that a significant portion of divalent counterions is transiently bound to the quaternary ammonium groups of the polyion with a lifetime that is lower than 1 ns. We call this process dynamic electrostatic attachment.[9]

Herein we raise the question whether such dynamic electrostatic attachment is also observable for a more weakly charged Ru^{II} coordination polymer in which the carriers of the twofold positive charges are sterically shielded by bulky terpyridine ligands. In particular, we use double electron-electron resonance (DEER) spectroscopy[10] to characterize the spatial distribution of dianionic spin probe molecules (Fremy's salt (FS), potassium nitrosodisulfonate, Scheme 1) on a length scale between 1.8 and 5 nm. As this length scale includes the separations of direct and next-neighbor ions of the coordination polymers, such experiments should provide a clear signature of site-attachment[6g] of the counterions along the backbone of the rodlike coordination polymer. By examining distance distributions of the spin-carrying counterions we should also be able to obtain a semiquantitative

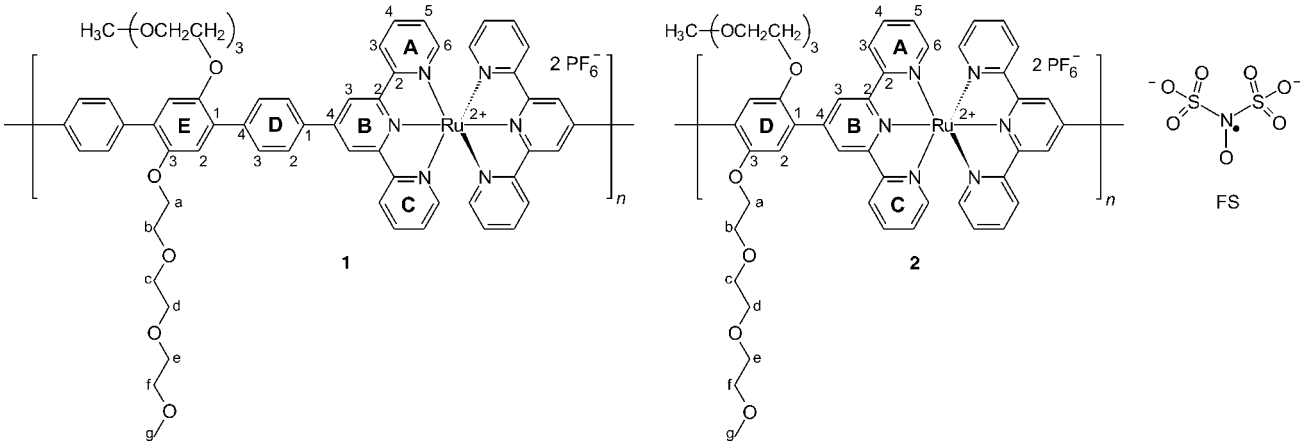

Scheme 1. Molecular structures of the spin probe FS (Fremy's salt) and the rodlike coordination polymers containing divalent ruthenium ions as charged groups (**1** and **2**), with the number of repeat units $n = 20–25$.

[*] Dr. D. Hinderberger, Priv.-Doz. Dr. G. Jeschke
Max-Planck-Institut für Polymerforschung
Postfach 3148, 55021 Mainz (Germany)
Fax: (+49) 6131-379-100
E-mail: jeschke@mpip-mainz.mpg.de
O. Schmelz, Prof. Dr. M. Rehahn
Deutsches Kunststoff-Institut (DKI) and
Ernst-Berl-Institut für Technische und Makromolekulare Chemie
Technische Universität Darmstadt
Petersenstrasse 22, 64287 Darmstadt (Germany)

[**] This work was supported by the Deutsche Forschungsgemeinschaft (Schwerpunktprogramm 1051 "High-Field EPR in Biology, Chemistry, and Physics"). We thank Manfred Schmidt for helpful discussions and Christian Bauer for technical support.

  DOI: 10.1002/ange.200460500

estimate of the extension of the counterion clouds around the charged groups.

The two ruthenium(II)-based coordination polymers **1** and **2** (Scheme 1) only differ in the separation of the Ru^{2+} centers along the backbone. Each Ru^{2+} center is electrostatically compensated by two PF_6^- counterions. It was estimated from NMR endgroup analysis that both compounds are built up of approximately 25 repeat units, and it was shown that these substances display macroscopic polyelectrolyte properties.[1f,g]

Experiments were performed on solutions of **1** (0.5 mM Ru^{2+} repeat units) and **2** (0.75 mM Ru^{2+} repeat units for pulse EPR, 0.6 mM Ru^{2+} repeat units for CW EPR) that contained an amount of spin-carrying FS counterions (0.5 mM) that approximately matched the number of Ru^{2+} centers. Solutions of **1** had to be prepared with a ternary solvent mixture of 50 vol% DMF and 50 vol% glycerol/water (1:1, v/v) since **1** is not very soluble in water and FS is not very soluble in DMF, while solutions of **2** and FS could be prepared in the binary solvent mixture of 33 vol% glycerol/67 vol% water (for pulse EPR) and 43.5 vol% glycerol/56.5 vol% water (for CW EPR). Addition of glycerol increases the viscosity and thus shifts rotational correlation times for FS dianions closer to the slow-tumbling regime where spectra are more sensitive to specifics of rotational diffusion. Furthermore, glycerol prevents crystallization of the solvent mixture during shock-freezing of the samples, so that glassy samples are obtained and precipitation of the coordination polymer can be avoided.

We first checked for the presence of interspin distances below 2 nm, which would lead to significant broadening in the low-temperature EPR spectra of the nitroxide group. While no such broadening is observed in the field-swept echo-detected EPR spectrum of FS anions in the presence of **1**, broadening in the wings of the spectrum is found in the presence of **2** (data not shown). As the distance between directly neighboring Ru^{2+} ions is longer than 2 nm in **1**, but significantly shorter than 2 nm in **2**, this finding would be consistent with some degree of attachment of FS dianions to the charged groups of the coordination polymers.

To test this hypothesis we have performed DEER experiments. Primary DEER signals of glassy frozen solutions FS with **1** and **2** are presented in Figure 1a and c, respectively. Both time traces clearly cannot be fitted by an exponential decay function (gray curve) as would be expected if the FS dianions were distributed homogeneously throughout the sample. In contrast, a time trace for the coordination monomer with the same spacer as in coordination polymer **2** can be fitted by an exponential decay function (data not shown). Furthermore, the shape of the two signal traces for **1** and **2** differs, which proves that the deviations from the homogeneous distribution are specific signatures of the structure of the coordination polymer.

Indeed the distance distributions obtained from these data by a model-free direct integral transformation[11] both exhibit two marked peaks that are situated at 2.4 and 4.7 nm for **1** (Figure 1b) and 2.9 and 4.5 nm for **2** (Figure 1d) and have approximately Gaussian shape. The additional weaker peak at approximately 3.5 nm in Figure 1b (asterisk) may be a noise artifact, as it is not observed in data with shorter maximum dipolar evolution times (not shown). We nevertheless discuss the data for longer maximum evolution times, as they provide a better estimate of the width of the peak at 4.7 nm.

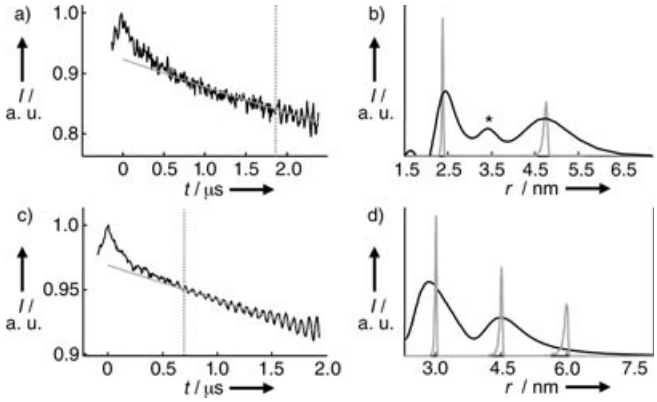

Figure 1. DEER time-domain data (a,c) and extracted distance distributions (b,d) of FS in solutions of **1** (a,b) in 50 vol% DMF/50 vol% glycerol/water and **2** (c,d) in 33 vol% glycerol/67 vol% water. The time traces were recorded at $T = 20$ K and gray lines are exponential fits to the data of FS/**1** between 1.9 and 2.4 μs and FS/**2** between 0.7 and 1.8 μs (both marked by the gray dotted line). The broad distance distributions (black lines) shown in (b) and (d) are obtained by integral transformation,[11] the overlaid gray lines are Ru···Ru distance distributions obtained from an MD simulation as explained in the text. Amplitudes of the MD distributions are scaled by a factor of 0.1. The asterisk in (b) marks a noise artifact.

Remarkably, in both cases the two distances correspond rather nicely to the expected distances between Ru^{2+} centers that are separated by one (peak at 2.4 nm for **1**), two (peak at 4.7 nm for **1** and peak at 2.9 nm for **2**), or three (peak at 4.5 nm for **2**) spacers. The distance of 1.5 nm expected for Ru^{2+} centers separated by one spacer in **2** cannot be reliably detected, as it coincides with an artifact arising from proton modulation.[10,11] This proton modulation is mainly a consequence of solvent protons. Differences in its depth may arise from the different solvent composition, but may also be caused by the slightly different timing of the two experiments. Distances longer than 5 nm cannot be extracted at the experimentally accessible maximum dipolar evolution times. The corresponding part of the distance distribution is suppressed by background correction of the primary data before the integral transformation.[11] This background correction was performed by fitting a monoexponential function to the data at $t > 1$ μs, which corresponds to the assumption of a homogeneous distribution of the FS ions in three dimensions at sufficiently long distances. The slightly stronger background decay for **1** relative to **2** reflects a higher local concentration of FS anions in the former polymer. Deviations from the selected background model cannot definitively be excluded. In particular, it is known that electrostatic repulsion between FS dianions causes an under-representation of short distances.[12] Furthermore, the elongated shape of the polymer chain breaks the spherical symmetry and might cause an admixture of a homogeneous distribution in only one dimension, as we observed earlier on a flexible polyelectrolyte with higher charge density.[9b] However, given the relatively low bulk concentrations, the corresponding contri-

butions to the decay function are hardly expected to exceed the noise level. When intentionally varying the background decay function we found only minor changes in the distance distribution that do no affect the conclusions drawn above.

The modulation depth obtained after dividing the data by the background function and renormalizing intensity at $t = 0$ contains information on the fraction of FS ions that are close to the coordination polymer. We can estimate that less than 20% of the Ru^{2+} ions have FS counterions attached. A more precise quantification is not possible on the basis of our data, as, in contrast to the distance distribution at $r < 5$ nm, the estimate of the modulation depth is rather sensitive to the choice of background function.

To obtain an estimate for the variation of the distances between the Ru^{2+} centers we performed molecular dynamics simulations in a vacuum for 2 ns of oligomers of both compounds end-capped with terpyridine moieties (**1**: two repeat units and two end caps, **2**: four repeat units and two end caps). The respective distance distributions are shown as solid gray lines in Figure 1 b,d. The theoretically predicted Ru···Ru distance distributions are much narrower than the extracted FS···FS distributions, while the maxima in the distribution (2.35 and 4.7 nm for **1**; 3 and 4.5 nm for **2**) are almost identical to those obtained from the direct DEER transformation.

We consider the latter finding as clear evidence for electrostatic attachment of at least a fraction of FS dianions to the charged groups on the coordination polymers. In the simple picture of (spherically symmetric) Coulomb interaction, such pairing is favored compared to the interaction with the original monovalent counterions of the polyion as it leads to a twofold increase in electrostatic interaction energy, and the replacement of monovalent counterions by divalent counterions is also favored by the gain in entropy for the system as a whole. Nevertheless, it is remarkable that electrostatic site attachment of counterions can be observed for relatively short, weakly charged polyions with approximately 25 repeat units and linear charge densities of the order of 1 nm^{-1}.

The larger width of the peaks in the experimental FS···FS distance distribution compared to the peaks in the theoretically predicted Ru···Ru distance distribution (**1**: full width at half maximum (FWHM) ca. 0.5 nm for the 2.4-nm peak and ca. 1 nm for the 4.7-nm peak; **2**: FWHM ca. 0.6 nm for the 2.9-nm peak and ca. 1 nm for the 4.5-nm peak) can be attributed to the sterical shielding of the Ru^{2+} ions by the terpyridine ligands and to the electrostatic nature of the localized attachment of the counterions. The upper part of Figure 2 shows (using **1** as an example) that if one assumes an octahedral symmetry around a Ru^{2+} center there are at least four equal positions of closest contact for FS counterions. The lower part of Figure 2 gives a schematic plot of the volume around polymer **1** in which FS ions are most likely to reside. Force-field calculations of the structure of both coordination polymers suggest side lengths of about 0.6 nm for the (hypothetical) square "box" that approximates the attachment volume around the Ru^{2+} site, that is, the spatial region in which FS ions can access the oppositely charged Ru^{2+} ions. This attachment volume effectively translates to a degree of freedom for the electrostatic attachment of FS to a Ru^{2+} center, which broadens the FS···FS distribution. Assuming a Gaussian distribution of ions in the attachment volume, such broadening has a square-root dependence on the number of spacers in between the Ru^{2+} centers, which would be consistent with the observed increase in width of the FS distance peak on going to longer distances.

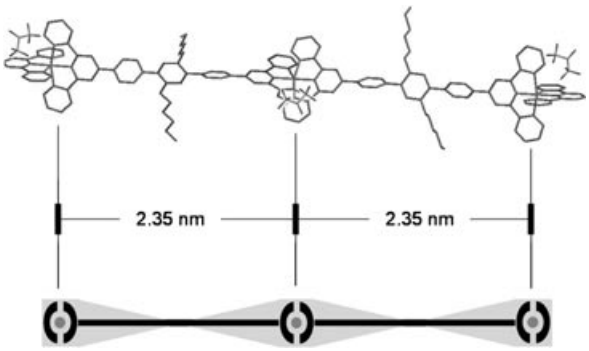

Figure 2. Schematic representation of possible localized binding of FS ions to Ru^{2+} centers in **1**. Top: An end-capped coordination dimer that has been geometry-optimized by force-field calculations (UFF 1.02) as explained in the text. The distinct distances between FS found from DEER data analysis (ca. 2.4 nm and ca. 4.7 nm) agree very well with the distances between Ru^{2+} centers separated by one or two organic spacers, respectively. Bottom: Schematic plot of most probable attachment sites for FS ions (gray area). The relatively broad distribution of spin probe distances can be explained if one accounts for the degrees of freedom of the electrostatic attachment.

The electrostatic origin of the FS distance distribution also accounts for the fact that FS distance peaks are indeed Gaussian-like and not asymmetric like the theoretical Ru···Ru distance peaks (see Figure 1 b,d). The asymmetry of the latter peaks reflects that the maximum distance upon bending an ideal rigid rod must be that of full linear extension, which is at the same time the most likely distance. Broadening of the peaks by diffuse electrostatic attachment makes this effect unobservable in the FS···FS distance distribution.

To probe the dynamics of the observed attachment process CW EPR spectroscopy was performed on fluid solutions of the same samples. Comparison of the spectra for solutions of only FS (Figure 3 a) and FS and **2** (Figure 3 b, black solid line) reveals a subtle but significant change in the relative intensities of the three lines of the spectrum of the nitroxide group. The same behavior was observed for a solution of **1** (data not shown).

In the spectrum of pure FS (Figure 3 a) the center-field line is the narrowest and has the highest relative amplitude, followed by the low-field line and the high-field line. This pattern is also observed for pure FS in all other solvents. In the spectrum of the solution with added **2** (1.5:1 Ru^{2+}:FS^{2-}), the low-field line is the narrowest and most intense, the center-field line is slightly less intense, and the high-field line is significantly further decreased in intensity. This change indicates that rotational diffusion of the FS dianions is significantly altered by the presence of the coordination polymer. To understand this change in rotational dynamics, spectral simulations were performed by using the program developed by Schneider and Freed[13] which can take into

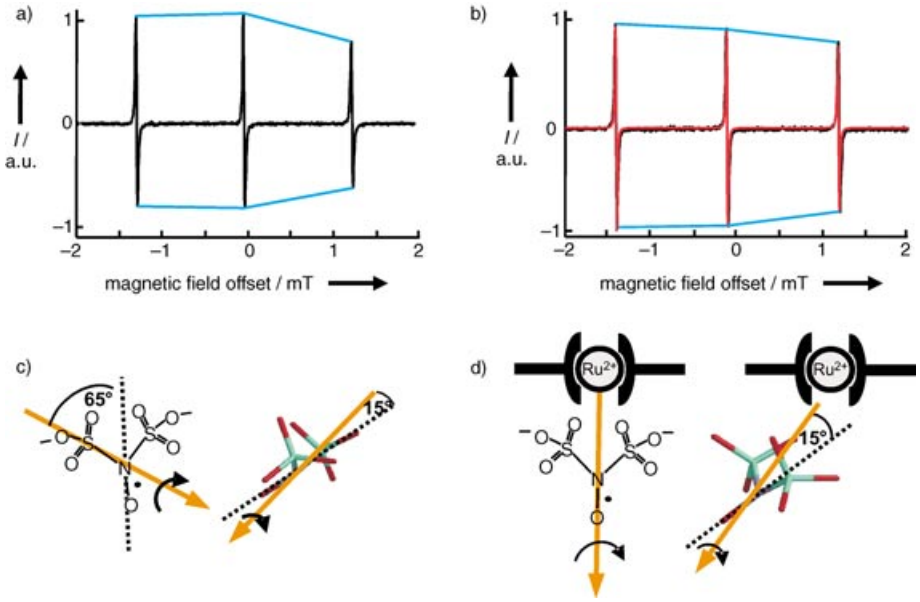

Figure 3. CW EPR spectra (X-band, ca. 9.8 GHz) at room temperature of a) 0.5 mM FS in 43.5 vol% glycerol/56.5 vol% water; b) 0.4 mM FS + 0.6 mM **2** (monomeric units) 43.5 vol% glycerol/56.5 vol% water. A spectral simulation of FS/**2** according to the rotational diffusion tensor explained in the text is shown in red. The blue lines are guides to the eye that pinpoint the change in relative amplitudes of the lines between (a) and (b). c) A visualization of the rotational diffusion tensor for FS in the solvent system 50 vol% glycerol/50 vol% water and d) displays the rotational diffusion tensor for FS with oppositely charged **2** in the same solvent; the orange arrows illustrate the principal axes of fast rotation of FS (c: 65° from the NO bond axis, see projection on the right and 15° out of plane of the plane ONS(2); d: 15° tilted away from the NO-bond axis, in the plane spanned by S(1)NS(2)). The principal values of the rotational diffusion tensor are for a) FS: $d_{\parallel}=30\times10^{9}\ s^{-1}$ (parallel to orange unique axis), $d_{\perp}=6\times10^{9}\ s^{-1}$ (perpendicular to orange axis), and for b) FS/**2**: $d_{\parallel}=30\times10^{9}\ s^{-1}$ (parallel to orange unique axis), $d_{\perp}=0.9\times10^{9}\ s^{-1}$ (perpendicular to orange axis).

account the effect of anisotropies in the rotational diffusion tensor. For simplicity, axial symmetry of the diffusion tensor was assumed.

The best simulation for free FS ions in pure solvents reproduces the lineshape pattern very well (simulation not shown in Figure 3a). It corresponds to a direction of the unique axis of the tensor of rotational diffusion along the N–S bond between the nitroxide group and one of the sulfonate groups (Figure 3c). In contrast, the simulation for the solution containing FS and **2** (red line in Figure 3b, slight deviation arising from phasing problems in the experimental spectrum) corresponds to a unique axis bisecting the two N–S bonds in the FS molecule (Figure 3d). This difference demonstrates that the divalent FS anions preferably interact with the polyion rather than with monovalent counterions, both in frozen solutions and also in fluid solutions.

Remarkably, rotational diffusion of the FS dianion in pure solvents is already slightly but significantly anisotropic, even though the shape of the molecule is almost spherical. The observation that rotation about the axis pointing to one sulfonate group is six times faster than rotation perpendicular to this axis (Figure 3c) can be explained by assuming that dynamic contact ion pairs are formed between one of the sulfonate groups and a counterion (K^+). For short times, the pair might then rotate as a whole about its long axis, which corresponds to the unique axis of the experimentally determined rotational diffusion tensor. The apparent symmetry breaking, that is, the favoring of one of two equivalent N–S bonds would result if on average only one or less contact with a counterion occurs on the timescale of the experiment (less than 1 ns).

This symmetry breaking does not occur in solutions of the coordination polymers where rotational diffusion preferably takes place about an axis bisecting the angle between both sulfonate groups (Figure 3d). Unlike monovalent potassium ions, the divalent Ru^{2+} ion thus appears to interact with both FS sulfonate groups simultaneously. The lifetime of such a "three-center ionic assembly" must be of the same order of magnitude as those of the ion pairs formed with monovalent ions, since the rotational diffusion rates are similar in both cases (about the unique axis $d_{\parallel}=30\times10^{9}\ s^{-1}$, perpendicular to the unique axis $d_{\perp}=0.9\times10^{9}\ s^{-1}$).

In conclusion, by applying two experimental techniques, CW EPR and DEER spectroscopy, to systems of spin-carrying counterions and oppositely charged, rodlike coordination polymers we could demonstrate that divalent counterions interact preferentially with the polyion and that their spatial distribution reflects the spatial distribution of charges on the polyion. We have found that the counterion cloud around bis(terpyridine)-coordinated transition-metal centers has an approximately Gaussian radial distribution with a width of approximately 0.5 nm. The electrostatic self-assembly underlying this spatial heterogeneity is a transient process in which the a lifetime of the electrostatically attached state is less than 1 ns.

Experimental Section

Fremy's salt of technical grade was bought from ICN Biomedicals and used as received.

1: A mixture of 2,5-bis(1,4,7,10-tetraoxaundecanyl)benzene-1,4-diboronic acid[14] (145 mg, 0.295 mmol, 1 equiv) and 4′-(*p*-bromophenyl)-2,2′:6′,2″-terpyridine[15] (229 mg, 0.590 mmol, 2 equiv) were refluxed under nitrogen in a mixture of THF (6 mL), water (6 mL), $NaHCO_3$ (760 mg, 9.047 mmol), and $[Pd(PPh_3)_4]$ (5.0 mg, 0.0043 mmol) for 48 h. After cooling the mixture down to room temperature, it was extracted with $CHCl_3$ (3 × 25 mL). The combined organic layers were dried ($MgSO_4$), the solvent was removed in vacuum, and the resulting yellowish solid was recrystallized from a mixture of methanol and chloroform (9:1; v/v).

$RuCl_3\cdot3H_2O$ (77.0 mg, 0.294 mmol) was activated by treatment with $AgBF_4$ (175.7 mg, 0.902 mmol) in acetone (25 mL).[11f] After removal of the precipitate (AgCl) by filtration, the solvent was removed in vacuo, and the resulting solid was dissolved in *N*,*N*-dimethylacetamide. The resulting black-violet solution was combined

with the above ligand monomer and then heated for 72 h at 130 °C. After cooling down the mixture to room temperature, it was poured into a saturated aqueous KPF_6 solution (900 mL). The red precipitate was separated by filtration, washed several times with water and dried in vacuo (P_4O_{10}); yield: 238 mg (57 %). ^{1}H NMR (500 MHz, [D$_6$]DMSO): $\delta = 3.21$ (m, 6H, H^g), 3.46 (m, 4H, H^f), 3.59 (m, 4H, H^e), 3.64 (m, 4H, H^d), 3.69 (m, 4H, H^c), 3.88 (m, 4H, H^b), 4.38 (m, 4H, H^a), 7.33 (m, 4H, H^{A5}), 7.40 (m, 2H, H^{E2}), 7.60 (m, 4H, H^{A6}), 7.97(m, 4H, H^{D3}), 8.14 (m, 4H, H^{A4}), 8.56 (d, 4H, H^{D2}), 9.17 (m, 4H, H^{A3}), 9.57 ppm (m, 4H, H^{B3}).

2: 4′-Bromo-(2,2′:6′,2″)-terpyridine[16] (187 mg, 0.60 mmol, 2 equiv) and 2,5-bis-(1,4,7,10-tetraoxaundecanyl)-phenyl-1,4-diboronic acid[15] (147 mg, 0.3 mmol, 1 equiv) were refluxed under nitrogen in a mixture of ethanol (1 mL), water (2 mL), toluene (3 mL), [Pd(PPh$_3$)$_4$] (10.0 mg, 0.0087 mmol, 1.4 mol %), and Na_2CO_3 (143 mg, 1.35 mmol, 4.5 equiv) for 48 h. After cooling down the mixture to room temperature, it was extracted with CH_2Cl_2 (3 × 25 mL). The combined organic layers were dried ($MgSO_4$) and the solvent was removed in a vacuum. The residue was purified by precipitation from dichloromethane solution using *n*-hexane (3 times). A yellow, highly viscous residue was obtained after drying in vacuum (P_4O_{10}). This ligand monomer was added to a solution of activated ruthenium in *N*,*N*-dimethylacetamide (20 mL), which was prepared as described above from $RuCl_3 \cdot 3H_2O$ (100 mg, 0.383 mmol) and $AgBF_4$ (228 mg, 1.169 mmol) in acetone (30 mL). The mixture was heated to 130 °C for 72 h and then cooled down to room temperature. A red precipitate was obtained by adding saturated aqueous NaCl (100 mL). The solid was isolated by centrifugation, dissolved in water, and precipitated by addition of saturated aqueous NaCl. The polymer was dried in vacuum (P_4O_{10}); yield: 196.3 mg (63.4 %). ^{1}H NMR (500 MHz, [D$_6$]DMSO): $\delta = 3.04$ (m, 6H, H^g), 3.23 (t, 4H, H^f), 3.35 (m, 4H, H^e), 3.53 (m, 4H, H^d), 3.73 (m, 4H, H^c), 4.09 (m, 4H, H^b), 4.71 (m, 4H, H^a), 7.41 (m, 4H, H^{A5}), 7.62 (m, 4H, H^{A6}), 8.07 (m, 4H, H,^{D2}), 8.17 (m, 4H, H^{A4}), 9.03 (m, 4H, H^{A3}), 9.55 ppm (m, 4H, H^{B3}).

Preparation of samples of FS/**1** and FS/**2** for pulse EPR spectroscopy and FS/**1** for CW EPR spectroscopy: Solvent mixtures were made from deionized Milli-Q-water, 87 wt % glycerol/water (Aldrich Chem. Co.) and DMF (Aldrich Chem. Co.). Stock solution of 2 mM FS in water was adjusted to about pH 8.5 by addition of KOH to enhance the stability of the Fremy's salt. This stock solution (25 μL) was added to a mixture of a solution of **1** in DMF (2 mM, 50 μL) and 87 % glycerol/water (25 μL) or to a mixture of a solution of **2** in water (2 mM, 37.5 μL) and 87 % glycerol/water (37.5 μL). In the case of **1**, a precipitate formed from the dark-red solution after a few minutes (this precipitate is assumed to be **1**, thus effectively reducing the concentration of **1**). Separation of the precipitate by use of a centrifuge gave a clear, light-red solution, which was subsequently used for the EPR measurements. No precipitate was found in solutions of FS and **2** in the binary glycerol/water solvent mixture.

Samples of FS/**2** for CW EPR spectroscopy: The same FS stock solution in water (25 μL) was added to a mixture of a 2 mM solution of **2** in water (30 μL) and 87 % glycerol/water (50 μL).

EPR studies: CW EPR spectra in solution ($T = 293$ K) at the X-band (ca. 9.8 GHz) were measured on a Bruker ELEXSYS 580 spectrometer with an AquaX inlet in a rectangular cavity (4103TM, Q values typically 3000). Four-pulse DEER time-domain signals at $T = 20$ K were obtained on the same spectrometer with a Bruker Flexline split-ring resonator (ER 4118X-MS3) with overcoupling to $Q \approx 100$ at a temperature of 20 K. The pulse sequence was $(\pi/2)_{\nu A} - \tau_1 - (\pi)_{\nu A} - t' - (\pi)_{\nu B} - (\tau_1 + \tau_2 - t') - (\pi)_{\nu A} - \tau_2$ echo, with a phase cycle $[(+x) - (-x)]$ applied to the first pulse, and τ_1 was averaged over 8 increments ($\Delta\tau_1 = 8$ ns) to suppress proton modulations.[10c,11] Here, ν_A is the observer frequency (local maximum at the low-field edge of the EPR absorption spectrum) and ν_B the pump frequency (global maximum of the EPR absorption spectrum, $\nu_B = \nu_A - 56$ MHz). The time t' after the first π pulse was incremented, the pulse lengths, and delays were as follows: $(\pi/2)_{\nu A} = 32$ ns, $(\pi)_{\nu A} = 32$ ns, $(\pi)_{\nu B} = 12$ ns, $\tau_1 = 200$ ns, $\tau_2 = 2.4$ μs (**1**) and $\tau_2 = 2$ μs (**2**), $\Delta t' = 8$ ns, $t'_0 = 80$ ns. The pump pulses were generated by feeding the output of a Magnettech OSC 101/1 sweep oscillator to one microwave-pulse-forming unit of the spectrometer. The repetition times were 6 ms (FS/**1**) and 3 ms (FS/**2**).

Data analysis: CW EPR spectral simulations were performed with a program by Schneider and Freed assuming a uniaxial tensor of rotational diffusion.[13] The following magnetic parameters were assumed. *G* tensor: $g_{xx} = 2.0086$, $g_{yy} = 2.0064$, $g_{zz} = 2.0029$; hyperfine tensor: $A_{xx} = A_{yy} = 0.525$ mT, $A_{zz} = 2.845$ mT; additional linewidth 4.6 μT. DEER time traces were analyzed by direct integral transformation, which has been reviewed elsewhere.[11]

Molecular dynamics simulations: Molecular dynamics simulations were carried out with the program package Cerius2 (version 3.8, Molecular Simulations, Inc.), using the UFF universal force field. The systems were first pre-equilibrated (canonical ensemble in a Berendsen temperature bath, 20000 steps, time step 0.5×10^{-15} s) and then sampled by a 2 ns run (Nosé-Hoover thermostat, 4×10^6 steps, time step 0.5×10^{-15} s). Structures were written to trajectory files in time intervals of 1×10^{-13} s. Time traces of the Ru coordinates were extracted from the trajectory files using the gOpenMol program and converted into histograms of the distance distribution by a home-written Matlab (The MathWorks, Inc.) program.

Received: April 29, 2004
Published Online: August 12, 2004

Keywords: coordination polymers · electrostatic interactions · EPR spectroscopy · noncovalent interactions · self-assembly

[1] a) J.-M. Lehn, *Angew. Chem.* **1990**, *102*, 1347 – 1362; *Angew. Chem. Int. Ed. Engl.* **1990**, *29*, 1303 – 1319; b) J.-M. Lehn, *Supramolecular Chemistry*, Wiley-VCH, Weinheim, **1995**; c) M. Rehahn, *Acta Polym.* **1998**, *49*, 201 – 224; d) H. Chen, J. A. Cronin, R. D. Archer, *Macromolecules* **1994**, *27*, 2174 – 2180; e) J.-P. Sauvage, J. P. Collin, J. C. Chambron, S. Guillerez, C. Coudret, V. Balzani, F. Barigelletti, L. De Cola, L. Flamigni, *Chem. Rev.* **1994**, *94*, 993 – 1019; f) S. Kelch, M. Rehahn, *Macromolecules* **1999**, *32*, 5818 – 5828; g) O. Schmelz, M. Rehahn, *e-Polym.* **2002**, no. 47; h) D. Wöhrle, A. D. Pomogailo, *Metal Complexes and Metals in Macromolecules*, Wiley-VCH, Weinheim, **2003**.

[2] a) J. Bohrisch, C. D. Eisenbach, W. Jaeger, H. Mori, A. H. E. Müller, M. Rehahn, C. Schaller, S. Traser, P. Wittmeyer, *Adv. Polym. Sci.* **2004**, *165*, 1 – 41; b) C. Holm, M. Rehahn, W. Oppermann, M. Ballauff, *Adv. Polym. Sci.* **2004**, *166*, 1 – 27; c) S. Förster, M. Schmidt, *Adv. Polym. Sci.* **1995**, *120*, 51 – 133; d) H. Dautzenberg, W. Jaeger, J. Kötz, B. Philip, C. Seidel, D. Stscherbina, *Polyelectrolytes—Formation, Characterization and Application*, Carl Hanser, Munich, **1994**.

[3] T. Pfohl, Y. Li, J. H. Kim, Z. Wen, G. C. L. Wong, I. Koltover, M. W. Kim, C. R. Safinya, *Colloids Surf. A* **2002**, *198–202*, 613 – 623.

[4] G. Decher, *Science* **1997**, *277*, 1232 – 1237.

[5] J. Kötz, S. Kosmella, T. Beitz, *Prog. Polym. Sci.* **2001**, *26*, 1199 – 1232.

[6] a) V. Vlachy, *Annu. Rev. Phys. Chem.* **1999**, *50*, 145 – 165; b) A. Y. Grosberg, T. T. Nguyen, B. I. Shklovskii, *Rev. Mod. Phys.* **2002**, 74, 329 – 345; c) M. Deserno, A. Arnold, C. Holm, *Macromolecules* **2003**, *36*, 249 – 259; d) G. S. Manning, *J. Chem. Phys.* **1969**, *51*, 924 – 933; e) G. S. Manning, *J. Chem. Phys.* **1969**, *51*, 934 – 938; f) G. S. Manning, *J. Chem. Phys.* **1969**, *51*, 3249 – 3252; g) G. S. Manning, *Acc. Chem. Res.* **1979**, *12*, 443 – 449.

[7] N. M. Atherton, *Principles of Electron Spin Resonance*, Ellis Horwood, New York, **1993**.

[8] A. Schweiger, G. Jeschke, *Principles of Pulse Electron Paramagnetic Resonance*, Oxford University Press, **2001**.
[9] a) D. Hinderberger, G. Jeschke, H. W. Spiess, *Macromolecules* **2002**, *35*, 9698 – 9706; b) D. Hinderberger, H. W. Spiess, G. Jeschke, *J. Phys. Chem. B* **2004**, *108*, 3698 – 3704; c) D. Hinderberger, H. W. Spiess, G. Jeschke, *Macromol. Symp.* **2004**, *211*, 71 – 86.
[10] a) A. D. Milov, A. G. Maryasov, Y. D. Tsvetkov, *Appl. Magn. Reson.* **1998**, 15, 107 – 143; b) R. G. Larsen, D. J. Singel, *J. Chem. Phys.* **1993**, *98*, 5134 – 5146; c) G. Jeschke, *ChemPhysChem* **2002**, *3*, 927 – 932.
[11] G. Jeschke, A. Koch, U. Jonas, A. Godt, *J. Magn. Reson.* **2002**, *155*, 72 – 82.
[12] A. D. Milov, Y. D. Tsvetkov, *Appl. Magn. Reson.* **2000**, *18*, 217 – 226.
[13] D. J. Schneider, J. H. Freed in *Biological Magnetic Resonance*, *Vol. 8* (Eds.: L. J. Berliner, J. Reuben), Plenum, New York, **1989**, chap. 1.
[14] S. Traser, P. Wittmeyer, M. Rehahn, *e-Polym.* **2002**, no. 32.
[15] P. Korall, A. Börje, P. O. Norrby, B. Åkermark, *Acta Chem. Scand.* **1997**, *51*, 760 – 766.
[16] B. Whittle, S. R. Batten, J. C. Jeffery, L. H. Rees, M. D. Ward, *J. Chem. Soc. Dalton Trans.* **1996**, 4249 – 4255.

